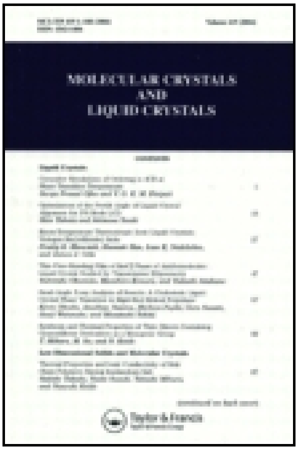

Molecular Crystals and Liquid Crystals

Publication details, including instructions for authors and subscription information:
http://www.tandfonline.com/loi/gmcl16

Molecular Reorientation in Liquid Crystals

J. A. Janik [a], M. Godlewska [b], T. Grochulski [c], A. Kocot [d], E. Sciesinska [b], J. Sciesisski [a] & W. Witko [a]

[a] Institute of Nuclear Physics, Kraków, Poland

[b] Institute of Physics, Jagiellonian University, Kraków, Poland

[c] Institute of Physics, Polish Academy of Sciences, Warszawa, Poland

[d] Institute of Physics, Silesian University, Katowice, Poland

To cite this article: J. A. Janik, M. Godlewska, T. Grochulski, A. Kocot, E. Sciesinska, J. Sciesisski & W. Witko (1983): Molecular Reorientation in Liquid Crystals, Molecular Crystals and Liquid Crystals, 98:1, 67-81

To link to this article: http://dx.doi.org/10.1080/00268948308073462

Mol. Cryst. Liq. Cryst., 1983, Vol. 98, pp. 67–81
0026-8941/83/9804–0067/\$18.50/0

Printed in the United States of America

Molecular Reorientation in Liquid Crystals[†]

J. A. JANIK,[‡] M. GODLEWSKA,[§] T. GROCHULSKI,[||] A. KOCOT,[¶]
E. ŚCIESIŃSKA,[§] J. ŚCIESIŃSKI,[‡] and W. WITKO[‡]

[‡]Institute of Nuclear Physics, Kraków, Poland; [§]Institute of Physics, Jagiellonian University, Kraków, Poland; [||]Institute of Physics, Polish Academy of Sciences, Warszawa, Poland; [¶]Institute of Physics, Silesian University, Katowice, Poland

(Received February 4, 1983)

The results of quasielastic neutron scattering (QNS) experiments for nematic and smectic liquid crystals performed in different laboratories are reviewed and compared with results of dielectric relaxation studies. The fIR spectra for PAA and HOAB in the frequency range of 20–200 cm^{-1} are presented. $\alpha(\bar{\nu})$ values for the nematic and isotropic phases in the whole frequency range including the microwave and submillimeter regions are discussed in terms of the two-time model for molecular librations in the potential cage (confined rotator model). The model fits very well all the experimental data obtained from microwave, carcinotron and fIR techniques. Additionally it may explain the discrepancy between QNS and dielectric relaxation correlation times.

I. INTRODUCTION

Comparison of Neutron and Dielectric Results

Many thermotropic liquid crystals were studied by the incoherent, quasielastic neutron scattering method (QNS) from the point of view of reorientational motions of molecules.

The Grenoble group mainly concentrated on various phases of TBBA.[1-10] The conclusion of these studies was: in the highly ordered smectic phases the molecules perform either 180° angular jumps around the long axes or a "biased" rotational diffusion with two minima around these axes; in the

---

[†] This paper was presented at Ninth International Liquid Crystal Conference in Bangalore, December 6–10, 1982, as an invited lecture.

less ordered smectic phases (H, C, A) as well as in the nematic phase the molecules perform a cylindrically symmetric rotational diffusion plus long axes fluctuations. The rotational diffusion (uniaxial) correlation times lie in the region $\sim 25 \div \sim 5$ ps. A much slower (10^{-8} s) reorientation around short molecular axes was not visible in the measurements.

The Exeter-Rutherford Laboratory group concentrated on

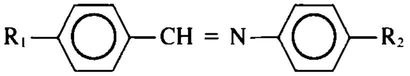

compounds.[11-17] The conclusion of these studies was: in the smectic E phases the molecules do not perform overall reorientations but only overdamped librations around the long axes; in the smectic B phases there are 180° angular jumps around long axes plus overdamped translational vibrations perpendicular to the smectic layers; in other smectic phases the molecules perform the rotational diffusion around long axes plus overdamped translational vibrations perpendicular to the smectic layers; in the nematic phases there is the rotational diffusion around long axes plus long axes fluctuations. The rotational diffusion (uniaxial) correlation times lie in the region ~ 80 ps–20 ps. Again, a much slower reorientation around short molecular axes was not visible in these studies.

The Kraków group concentrated on

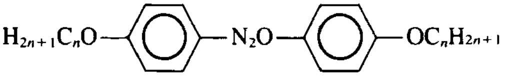

compounds.[18-22] The conclusion of these studies was: the rotational diffusion of molecules around long axes takes place in the smectic C phase ($n = 7$) and in the nematic phases ($n = 1$, 2 and 7). The rotational diffusion (uniaxial) correlation times lie in the region ~ 15 ps–ca. 5 ps. A much slower reorientation around short axes was not visible in these experiments.

It should be mentioned that all conclusions quoted and summarized above concern substances with deuterated end groups and therefore concern the body motions, as deuteration means masking for QNS incoherent experiments.

The substances studied by the Kraków group were also studied by the dielectric relaxation method. This method is powerful as it covers the whole range of frequencies from radio to microwave ones, which means also the very large range of relaxation times from 10^{-3} sec to 10^{-11} sec. The dielectric relaxation method detects in this way both: the reorientational motion of liquid crystal molecules around short axes (MHz technique) and the reorientational motion around long axes (GHz technique). The latter ones were indeed detected in substances studied by the Kraków group by

QNS, as well as in many other liquid crystal substances not yet investigated by neutrons.[23-28] The conclusions of all these microwave dielectric studies are: the dielectric relaxation times for reorientational motions around long molecular axes lie in the region of 10^{-10} sec for most of liquid crystal substances, but for those with short end groups they lie in the region of 10^{-11} sec. This statement is valid for nematics and less ordered smectics; for highly ordered smectics the dielectric relaxation times shift beyond 10^{-10} sec.

It is now time to give a quantitative comparison between the QNS and dielectric relaxation studies. Apart from the three liquid crystal substances studied by the Kraków group, all other liquid crystals were studied from the point of view of reorientation around long axes only either by QNS or by the dielectric method. The comparison is presented in Table I.

Two comments shall be made in connection with this Table I. Firstly, although the neutron determined correlation times were obtained by fitting to the data the uniaxial rotational diffusion model, a comparably good fit could be obtained by fitting the 180° angular instantaneous jump model — in this case with slightly shorter correlation (or rather residence) time values. Secondly, the dielectrically determined correlation times are simply the dielectric relaxation times, which implies an assumption that the internal field correlation factor and that converting the polymolecular response into the monomolecular one are equal to 1; apart from errors arising from this assumption the two sets of values should be respectively equal as the same physical quantities properly defined.

TABLE I

Comparison between QNS and dielectric relaxation times.

Substance	Neutron determined diffusion correlation time	Dielectrically determined uniaxial diff. correlation time	Ref.
Di-methoxyazoxybenzene (PAA) nematic, 398 K	4 ps	22 ps	18,23
Di-ethoxyazoxybenzene (PAP) nematic, 413 K	6 ps	30 ps	22,24
Di-heptyloxyazoxybenzene (HOAB) nematic, 378 K	12 ps	110 ps	21,25
Di-heptyloxyazoxybenzene (HOAB) smectic C, 359 K	12 ps	200 ps	21,25

It is evidently not so, as the neutron determined correlation times are significantly shorter than the dielectrically determined ones. Therefore, a suspicion arises, that the neutron determined times may not be a characteristic measure for the uniaxial rotational diffusion but something else. As a matter of fact we have mentioned already that the neutron determined times may appear nearly equal independent from whether they are understood as "rotational diffusion times," i.e. (approximately) times for reorientation by 1 radian or as "residence times" between instantaneous jumps. Moreover, it should be pointed out that if the neutron determined times were the rotational diffusion ones we would be facing another difficulty, connected namely with the fact that the time needed for reorientation around long axis by 1 radian via *free rotation* is nearly the same, which is very improbable.

Taking all these facts into account we propose the following mechanism of molecular reorientations around long axes in liquid crystals.

The molecule reorients around the long axis only when the neighboring molecules move translationally apart thus making enough room for the reorientation. In such situations the molecule performs a uniaxial rotational diffusion. The average duration of such situation let be t_1. Alternatively, the molecule remains in a "clutched" situation in which it cannot reorient but only performs librations around the long axis. The average duration of such situation let be t_2 (residence time). *Both* t_1 and t_2 are responsible for the shape of the QNS peak (see equations in Ref. 29), giving rise to *two* QNS components—the shorter t corresponding to the broader one. We believe that in all QNS experiments with liquid crystals discussed above, t_2 is smaller than t_1, although it is not negligibly small, which would correspond to a rotational diffusion. Therefore, we believe that what we understood so far as neutron determined rotational (uniaxial) diffusion correlation times should be reinterpreted as the times of residence during which the molecule performs libration around the long axis. The other time t_1 may give rise to a narrower QNS component, perhaps nondetectable with the resolutions applied.

If our suggestion is reasonable we should be able to observe the effect of librations of the molecule around the long axis as well as the effect of a finite duration of these librations via the Poley absorption band which should be visible in far infrared. Therefore, we are carrying out systematic fIR measurements with liquid crystals with the aim to compare the results with both the neutron (QNS) and the dielectric relaxation experiments. The first, preliminary results are presented in the next section.

II. FIR EXPERIMENTAL AND RESULTS

The far infrared (fIR) absorption spectra of PAA and HOAB in the range of 20–200 cm^{-1} were obtained using the vacuum version of the Digilab FTS-14 Fourier spectrometer.* The measurement resolution was 2 cm^{-1}. The spectra obtained were smoothed afterwards by the Digilab software smoothing procedure giving the effective resolution of 4 cm^{-1}. The smoothing does not distort any significant features of the band's shape. The number of scans, for both the samples and the references, was between 1000 and 3000. α-Quartz windows were used for the sample holder. The windows were oriented with respect to the considerably polarized beam in the instrument in order to get minimum window absorbance due to the quartz band at ca 120 cm^{-1}. The reference measurements were performed at temperatures relevant to the temperatures of sample measurements. Teflon or In spacers were used to seal the sample holder. Effective spacers thicknesses were established from the thicknesses of the sandwiches: window-spacer-window after the sample holder had been screwed. In the case of nematic PAA an adequate thermal treatment of the sample was applied to obtain a monodomain sample in order to avoid additional beam attenuation due to the scattering at domain boundaries. In order to avoid interference between the windows (channel effect) caused by the relatively high refractive index of quartz the two surfaces of one of the windows were ultrasonically shaped in a special way. That gave a nonflat sample and, in order to be able to derive correct absolute values of the absorption coefficient, measurements with different spacers were performed. We believe that this experimental procedure enabled us to get relatively reliable absolute values of absorption, which is confirmed by the fact that fIR measurements fit well the α values obtained in the 2 cm^{-1} – 13 cm^{-1} region by the use of the carcinotrons technique.

A review of the obtained fIR absorption spectra in the region of 20–200 cm^{-1} is presented in Figures 1–5. Those figures also include preliminary results for the crystalline and smectic phases.

Figure 1 shows an evolution of the PAA spectra at the nematic-isotropic phase transition. The peak position of the isotropic phase agrees with that reported by Venugopalan and Prasad.[32] Also, as they stated, the overall

---

*The cooperation with the Institute of Material Science Academy of Mining and Metallurgy, Kraków, which made possible these measurements is gratefully noted.

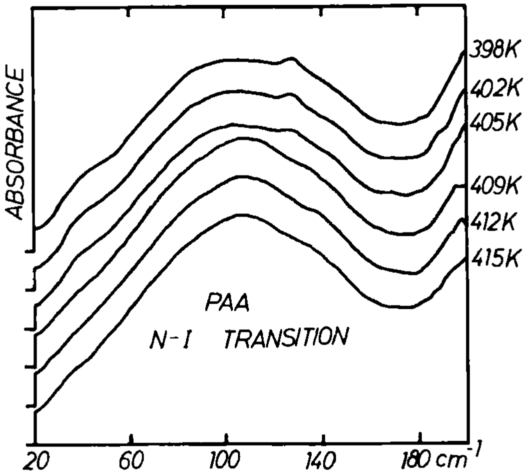

FIGURE 1 The evolution of PAA spectra at the nematic-isotropic phase transition.

shape of the spectra for isotropic and nematic phases is pretty similar. However, a small but evident change of the peak intensity at the phase transition is observed. This change (higher intensity for isotropic phase) is a feature of the phase transition and is not influenced by the radiation scattering, because, as already mentioned, the PAA nematic sample was a monodomain one.

The isotropic-nematic phase transition for HOAB is shown in Figure 2. In that case the nematic sample became "polydomain" one. Thus the apparent intensity change is strongly influenced by the scattering.

From Figure 3 it can be noticed that, for both PAA and HOAB, a weak and relatively narrow band appears in the nematic phase at 124 cm^{-1}. This peak, which may be treated as a "nematic phase detector", will not be discussed in the present paper.

The shape of the HOAB isotropic phase spectra varies considerably from that reported by Venugopalan and Prasad. It can be seen from our measurements (Figures 2, 3, 5) that the long-wavelength spectrum of that substance consists of at least two broad overlapping bands. We dare claim that our own experimental conditions were more suitable for giving evidence of this feature. An attempt to interpret such a shape of the HOAB spectrum will be given.

III. DISCUSSION

The application of fIR spectroscopy and submillimeter spectroscopy (carcinotron technique) enables one to determine the absorption coefficient

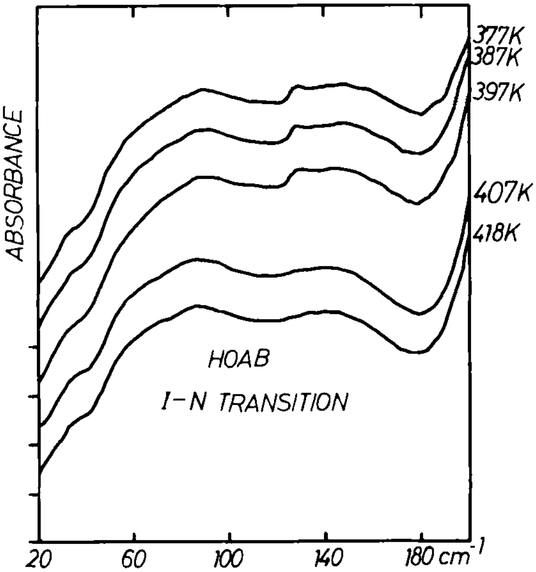

FIGURE 2 The evolution of HOAB spectra at the isotropic-nematic phase transition.

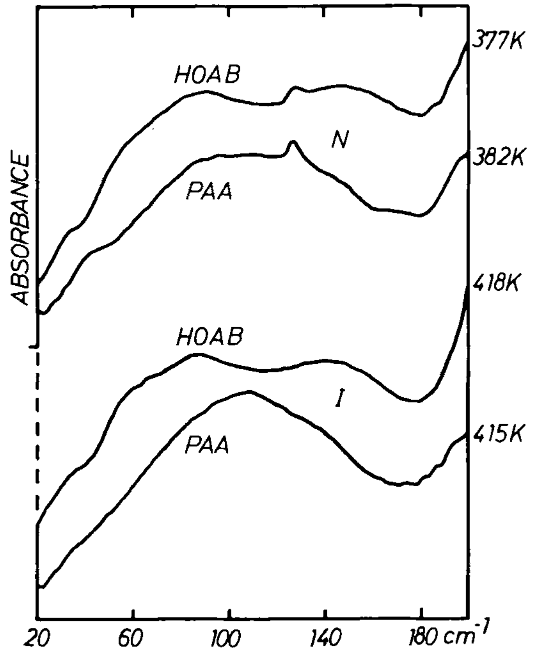

FIGURE 3 The comparison of HOAB and PAA spectra for the isotropic and nematic phases.

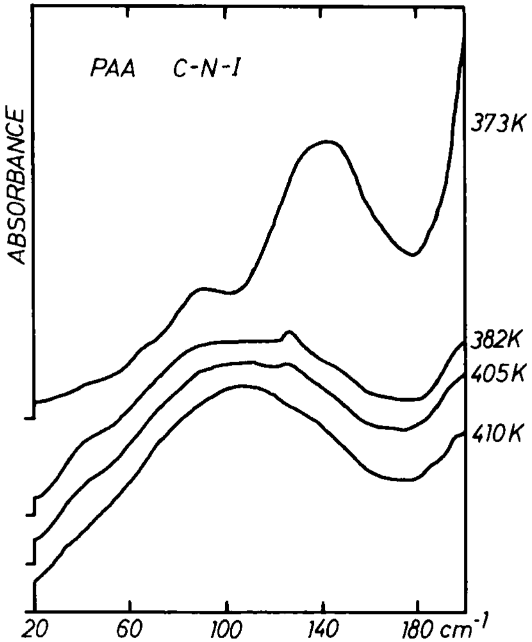

FIGURE 4 The PAA spectra for isotropic, nematic and crystalline phases.

$\alpha(\nu)$. In both cases the sample spectrum $I_s(\nu)$, background $I_0(\nu)$ and the sample thickness should be known. Then $\alpha(\nu)$ is defined as

$$\alpha(\nu) = \frac{1}{L} \ln \frac{I_0(\nu)}{I_s(\nu)}. \tag{1}$$

Since the measurements were performed for several sample thicknesses, the difference of the thicknesses ΔL was sufficient. The errors of $\alpha(\nu)$ determination are estimated to be smaller than 15% for the range from 20 cm^{-1} to 200 cm^{-1} and 4% for the range from 1.8 cm^{-1} to 13 cm^{-1}.

The frequency dependence of the absorption coefficient for isotropic and nematic phases of PAA is shown in Figure 6. The results for isotropic and nematic phases of HOAB are presented in Figure 7. For the microwave region $\alpha(\nu)$ was calculated from the formula

$$\alpha(\nu) = \frac{2\nu}{c}[(\varepsilon'^2(\nu) + \varepsilon''^2(\nu))^{1/2} - \varepsilon'(\nu)]^{1/2}, \tag{2}$$

where the electric permittivities $\varepsilon'(\nu)$ and $\varepsilon''(\nu)$ were taken.[23,25] The experimental values of the loss factor $\varepsilon''(\nu)$ in the 1.8–200 cm^{-1} range were

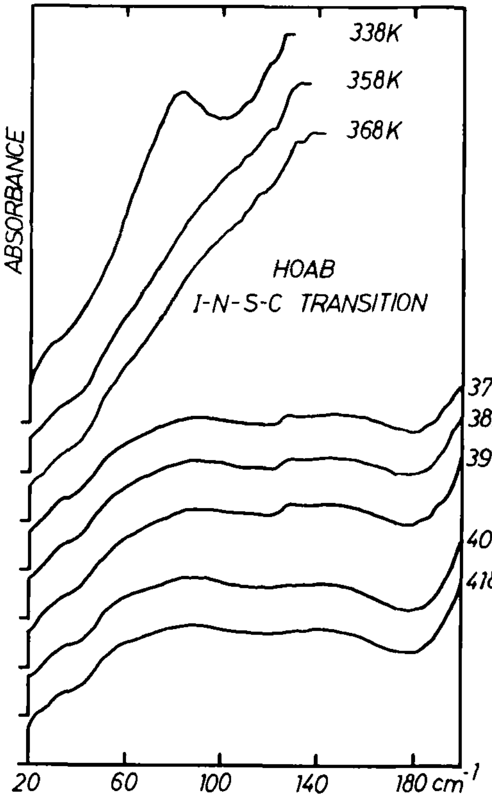

FIGURE 5 HOAB spectra for the isotropic, nematic, smectic and crystalline phases.

calculated from the relation $\varepsilon''(\nu) = \alpha(\nu)cn(\nu)\nu^{-1}$, assuming that the refractive index n is frequency independent and equals ca 1.7 for PAA and 1.6 for HOAB. From Figures 6 and 7 it is evident that the agreement of the results from different experimental techniques is good. There is no discrepancy between fIR and submillimeter spectroscopy in the range of 10–20 cm^{-1} and submillimeter spectroscopy and microwave results in the range of 1–2 cm^{-1} are also in good agreement.

In the case of PAA the maximum of $\alpha(\nu)$ appears at ca 105 cm^{-1}. We assume that this maximum is connected mainly with libration of molecule around the long molecular axis. Librations around the short molecular axes should appear at much lower frequencies, thus giving rise to weak absorption as the moment of inertia for that motion is over 10 times larger.

For an estimation of the librational contribution to absorption the experimental value of integral absorption A_{exp} should be compared with its the-

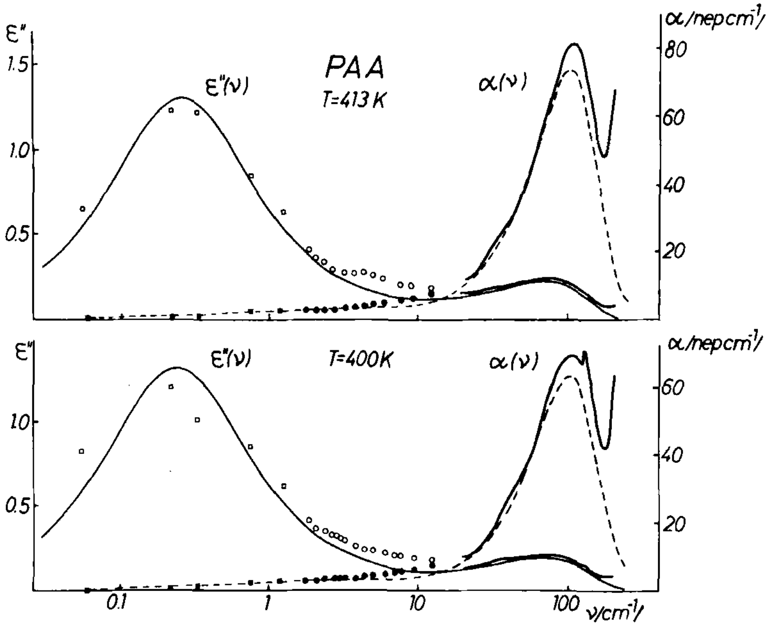

FIGURE 6 Absorption coefficient α and loss factor ε'' as a function of wavenumber ν (cm^{-1}) for PAA isotropic ($T = 413$ K) and nematic ($T = 400$ K) phases. Experimental results: fIR (heavy line), submillimeter spectroscopy (open dots for ε'' and filled dots for α values) and microwave data[23] (open for ε'' and filled squares for α values). Confined rotator model: α (dashed line) and ε'' (light line) bandshape for fitting parameters given in Table II.

oretical prediction A_{th}. It is seen in Figure 1 that there is a strong internal mode band at ca 210 cm^{-1} seriously disturbing the librational band profile on the high frequency side. Thus to omit this effect the A_{exp} value was derived from Eq. (3) under the assumption of the symmetric profile of the band around its maximum.

$$A_{\mathrm{exp}} = \frac{V}{N}\int_0^{+\infty} \alpha(\nu)\,d\nu = 2\frac{V}{N}\int_0^{\nu_{\max}} \alpha(\nu)\,d\nu, \tag{3}$$

where V/N is volume per one molecule.

For the nematic phase of PAA this estimation gives $A_{\mathrm{exp}} = 3 \times 10^{-18}$ cm. The value of A_{th} was calculated from the Gordon sum rule[33] with Polo-Wilson modification[34]

$$A_{\mathrm{th}} = \frac{(n^2+2)^2}{9n}\,\frac{\mu^2}{12\,c^2 I \varepsilon_0}, \tag{4}$$

where $\varepsilon_0 = 8.85 \times 10^{-12}$ F.m, μ–dipole moment, I–moment of inertia for the long axis.

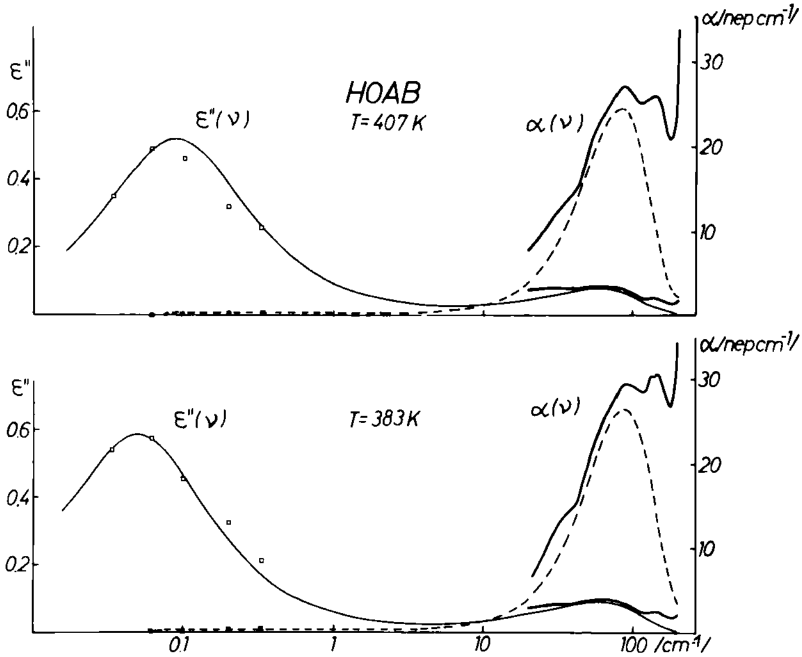

FIGURE 7 Absorption coefficient α and loss factor ε'' as a function of wavenumber ν (cm^{-1}) for HOAB isotropic (T = 407 K) and nematic (T = 383 K) phases. Notation as in Figure 6, microwave data from Ref. 25.

For the nematic phase of PAA A_{th} calculated with I and μ values[35,36] is equal to 2.4×10^{-18} cm. Thus the A_{th} is equal to 85% of A_{exp} value. A similar result is common for simple molecular liquids.[37,38]

There are some doubts as to the 105 cm^{-1} band assignment in PAA.[32,39,40] Some authors suggest that the contribution of torsional internal motion dominates there. However, the agreement of $A_{\text{th}}/A_{\text{exp}}$ ratio for PAA and simple liquids enables us to conclude that the 105 cm^{-1} band of PAA originates mainly from libration (Poley absorption).

An interpretation of fIR spectrum of HOAB is more complicated. There are two absorption bands (ca 85 and 140 cm^{-1}) and it seems that only one (85 cm^{-1}) originates from the libration around the long molecular axis. This libration should appear at a frequency lower than that for PAA, as the ratio of moments of inertia for both molecules is $(I_H/I_P)^{1/2} = 1.3$. The experimental frequency ratio for the 85 cm^{-1} band $\nu_P/\nu_H = 1.2$ is reasonable. For the 140 cm^{-1} band this ratio equals to 0.8, so this band cannot be assigned to libration. It should be connected with the internal deformational vibration. Its appearance at such a low frequency in comparison to PAA is due to the length of terminal alkyl chains.

For HOAB, A_{exp} and A_{th} were calculated in the same way as for PAA giving the values of 2.1×10^{-18} and 1.3×10^{-18} cm for A_{exp} and A_{th}, respectively. The ratio of 62% is still reasonable, proving small influence of the overlapping of other bands and of the induced absorption.

For both the PAA and HOAB spectra it is impossible to separate pure rotational bandshapes and to calculate the experimental correlation functions. The model calculation fittings can be carried out instead. The confined rotator model reproducing the spectra fairly well both in fIR and microwave regions for many liquids developed recently by Gajduk and Kalmykov,[41] was applied in this paper. In this model a two-dimensional rotator librates in the potential cage formed by its neighbors and reflects elastically from the walls. The rectangular cage of the width of 2β exists for a time interval and then the local configuration and angular momentum change instantaneously. This means that the other cage of the same size is formed, but with different orientation. For the lifetime distribution the Poisson distribution function with average lifetime τ was taken. Initial orientations of molecules are given by the Debye distribution function with characteristic time τ_D. The last assumption is equivalent to treating the motion of the cage as rotational diffusion. So, this model introduces three independent parameters: β, τ and τ_D. The formula for normalized complex permittivity is the following:[41]

$$\frac{\varepsilon^*(\omega) - n_\infty^2}{\varepsilon_s - n_\infty^2} = \left[1 + \frac{\tau_D}{\tau(1 - i\omega\tau_D)}\right] \frac{\sum_{n=1}^{\infty} S_n(f)\psi(z_n)}{\sum_{n=1}^{\infty} S_n(f)\psi(iy_n)(1 + \tau_D/\tau} \tag{5}$$

where subscripts s and ∞ denote low and high frequency limit, $f = 2\beta/\pi$ and the complex frequency $z_n = x_n + iy_n$ is defined as $x_n = \eta\omega f/n$ and $y_n = \eta f/\pi n$ where $\eta = (I/2\mathrm{kT})^{1/2}$. The weight function $S_n(f)$ of expansion in terms of thermal rotational harmonics $\psi(z_n)$ and these harmonics $\psi(z_n)$ are given by formulas (6) and (7), respectively

$$S_n(f) = \frac{8}{\pi^2} \frac{\sin^2[(\pi/2)(n - f)]}{(n^2 - f^2)^2}, \tag{6}$$

$$\psi(z) = 1 + i\pi^{1/2} z \exp(-z^2) \left[1 + \frac{2i}{\pi^{1/2}} \int_0^z \exp(t^2)\, dt\right], \tag{7}$$

The value of τ_D can be determined independently from microwave measurements and two other parameters of the model τ and β are adjusted for the best fit to the observed maximum of absorption $\propto_{max}$ and frequency ν_{max}, respectively. Therefore Gajduk's model contains two time parameters: τ and τ_D, where τ describes the time of the unperturbed libration and τ_D the time of the reorientation of the cage.

Applying the confined rotator model to our measurements we used experimental data for ε_s, n and τ_D from Refs. 23 and 25. For the value of $\alpha_{\max}$ we have taken 90% of experimental value, assuming that 10% is due to the induced absorption and overlapping of other bands. The values of $\alpha_{\max}$, $\nu_{\max}$, τ_D and the fitted parameters τ and β are presented in Table II. The final results of the fitting procedure for both $\alpha(\nu)$ and $\varepsilon''(\nu)$ are shown in Figures 6 and 7. The most important result of the model calculations is that the times of unperturbed libration τ for both PAA and HOAB are close to the correlation time from the QNS results presented in Table I. It is also seen that the reproduction of the bandshape in the whole fIR, submillimeter spectroscopy and microwave region is very good.

IV. CONCLUSIONS

It was shown that the shape of what we assumed to be the Poley absorption band for two liquid crystals investigated, PAA and HOAB, can be described by a model with *two* characteristic times: the Debye relaxation time and the duration time of librations. As the Debye relaxation time was taken from the microwave dielectric measurements, the fitting procedure to which the Poley absorption band was subjected provided the duration time to librations. This time of libration happens to be very near to the neutron determined time parameter thus indicating the correctness of the assumption stated at the end of Section 1, concerning a possible reinterpretation of neutron (QNS) data.

Two remarks have to be made in this connection: Firstly, we do not believe that the reinterpretation in question will lead to a change in conclusions concerning the "geometry" of molecular motions, especially those

TABLE II

Confined rotator model: PAA and HOAB experimental and fitting parameters.

Substance		T (K)	τ_D (10^{-12} s)	$\alpha_{\max}$ (nep cm^{-1})	$\nu_{\max}$ (cm^{-1})	τ (10^{-12} s)	β
PAA	isotropic	413	20	74	105	2.2	0.13
	nematic	400	22	62	105	2	0.13
HOAB	isotropic	403	60	24	85	7	0.12
	nematic	387	110	26	88	11	0.11

summarized in Section 1 as conclusions of the Grenoble group or the Exeter-Rutherford Laboratory group (the reinterpretation concerns only the correlation times). Secondly, one may expect that in some liquid crystals, those with the short end groups like PAA and PAP, the narrow component connected with reorientational time will be visible in QNS experiments; as the dielectric relaxation times (20–30 ps) are within the range of a good resolution QNS experiment. Hence, the good resolution QNS data for PAP should be subjected to model fittings with *two* time parameters. This does not apply to other liquid crystals where the corresponding dielectric times are of the order of 10^{-10} s, thus lying outside the scope of any QNS experiment. In those cases a *single* time fitting should be sufficient, but with a new interpretation of the characteristic time.

It should then be pointed out that the two times model was recently applied to the plastic phase of neopentane[30,31] with the aim to obtain a "unified" understanding of the QNS[29] and Raman scattering results.

Finally, we want to say that we are performing systematic studies by all three methods (QNS, dielectric relaxation, fIR) for other liquid crystals with the aim to collect more data that would support that "unified" understanding.

Acknowledgments

The authors would like to thank Professor K. Leibler and Professor E. Kluk for their interest and stimulating discussions.

The help of Dr. F. Maniawski and B. van Laar in preparation of quartz windows for fIR is highly appreciated.

References

1. H. Hervet, F. Volino, A. J. Dianoux and R. E. Lechner, *J. Phys. (Paris) Lett.*, **35**, 151 (1974).
2. A. J. Dianoux, F. Volino, A. Heidemann and H. Hervet, *J. Phys. (Paris) Lett.*, **36**, 275 (1975).
3. H. Hervet, F. Volino, A. J. Dianoux and R. E. Lechner, *Phys. Rev. Lett.*, **34**, 457 (1975).
4. A. J. Dianoux, A. Heidemann, F. Volino and H. Hervet, *Mol. Phys.*, **32**, 1521 (1976).
5. F. Volino, A. J. Dianoux and H. Hervet, *J. Phys. Colloq. (Orsay, Fr.)*, **37**, 55 (1976).
6. F. Volino, A. J. Dianoux and H. Hervet, *Solid State Commun.*, **18**, 453 (1976).
7. F. Volino and A. J. Dianoux, *Mol. Phys.*, **36**, 389 (1978).
8. A. J. Dianoux and F. Volino, *J. Phys.*, **40**, 181 (1979).
9. A. J. Dianoux, H. Hervet and F. Volino, *J. de Phys. (Paris)*, **38**, 809 (1977).
10. F. Volino, A. J. Dianoux and A. Heidemann, *J. Phys. (Paris) Lett.*, **40**, 583 (1979).
11. A. J. Leadbetter, R. M. Richardson, and C. J. Carlile, *J. Phys. Colloq. (Orsay, Fr.)*, **37**, 65 (1976).
12. A. J. Leadbetter and R. M. Richardson, *Mol. Phys.*, **35**, 1191 (1978).
13. R. M. Richardson, A. J. Leadbetter and J. C. Frost, *Ann. Phys.*, **3**, 177 (1978).
14. R. M. Richardson, A. J. Leadbetter, C. J. Carlile and W. S. Howells, *Mol. Phys.*, **35**, 1697 (1978).
15. D. H. Bonsor, A. J. Leadbetter and F. P. Temme, *Mol. Phys.*, **36**, 1805 (1978).

16. A. J. Leadbetter, R. M. Richardson and J. C. Frost, *J. Phys. Colloq. (Orsay, Fr.)*, **40**, 125 (1979).
17. A. J. Leadbetter, R. M. Richardson, B. A. Dasannacharya and W. S. Howells, *Chem. Phys. Lett.*, **39**, 501 (1976).
18. J. A. Janik, J. M. Janik, K. Otnes, J. Krawczyk and K. Rościszewski, *Physica*, **92B**, 351 (1977).
19. J. A. Janik, J. Krawczyk, J. M. Janik and K. Otnes, *J. Phys. Colloq. (Orsay, Fr.)*, **40**, 169 (1979).
20. J. A. Janik, Proc. Bangalore Conf. (1979).
21. J. A. Janik, J. M. Janik, J. Krawczyk and K. Otnes, *Mol. Cryst. Liq. Cryst.*, submitted (1982).
22. J. A. Janik, J. M. Janik, J. Krawczyk and K. Otnes, to be published (1983).
23. S. Wróbel, J. A. Janik, J. K. Mościcki and S. Urban, *Acta Phys. Pol.*, **A48**, 215 (1975).
24. S. Urban, S. Wróbel, K. Chłędowska, J. Chruściel, J. A. Janik and H. Kresse, paper presented at 9 ILCC, Bangalore, December 6–10.
25. X. P. Nguyen, S. Urban, S. Wróbel and H. Kresse, *Acta Phys. Pol.*, **A54**, 617 (1978).
26. J. P. Parneix, A. Chapoton and E. Constant, *J. de Phys.*, **36**, 1143 (1975).
27. M. Massalska-Arodź, J. K. Mościcki and S. Wróbel, *Acta Phys. Pol.*, **A58**, 443 (1980).
28. H. Kresse, D. Demus, S. Wróbel, J. K. Mościcki and S. Urban, *Acta Phys. Pol.*, **A57**, 699 (1980).
29. K. E. Larsson: *J. Chem. Phys.*, **59**, 4612 (1973).
30. Ph. Depondt, M. Debeau and R. M. Pick, *J. Chem. Phys.*, **77**, 2779 (1982).
31. Ph. Depondt and M. Debeau, *J. Chem. Phys.*, **77**, 30 (1982).
32. S. Venugopalan and S. N. Prasad, *J. Chem. Phys.*, **71**, 5293 (1979).
33. R. J. Gordon, *J. Chem. Phys.*, **38**, 1729 (1963).
34. S. R. Polo and M. K. Wilson, *J. Chem. Phys.*, **23**, 2376 (1955).
35. V. N. Tsvetkov and V. Marinin, *Zh. Eksp. Teor. Fiz.*, **18**, 641 (1948).
36. B. J. Bulkin and F. T. Prochaska, *J. Chem. Phys.*, **54**, 635 (1971).
37. A. Gershel, I. Darmon and C. Brot, *Mol. Phys.*, **23**, 317 (1972).
38. M. Benson, G. D. Martin, S. Walker, J. Warren and R. Wilson, *Can. J. Chem.*, **50**, 2610 (1972).
39. B. I. Bulkin and W. B. Lok, *J. Phys. Chem.*, **77**, 326 (1973).
40. A. Gruger, N. le Calvé and F. Romain, *J. Mol. Struc.*, **21**, 97 (1974).
41. V. I. Gajduk and Y. P. Kalmykov, *J. Chem. Soc., Faraday Trans.*, 2, **77**, 929 (1981).